AD_____

Award Number: W81XWH-11-2-0109

TITLE: Towards Development of a Field-Deployable Imaging Device for TBI

PRINCIPAL INVESTIGATOR: Pierre D. Mourad, Ph.D.

CONTRACTING ORGANIZATION: University of Washington
Seattle, WA 98107

REPORT DATE: March 2012

TYPE OF REPORT: Annual

PREPARED FOR: U.S. Army Medical Research and Materiel Command
Fort Detrick, Maryland 21702-5012

DISTRIBUTION STATEMENT: Approved for Public Release;
Distribution Unlimited

REPORT DOCUMENTATION PAGE

Form Approved
OMB No. 0704-0188

1. REPORT DATE	2. REPORT TYPE	3. DATES COVERED
March 2012	Annual	15 February 2011 – 14 February 2012

4. TITLE AND SUBTITLE

Towards Development of a Field-Deployable Imaging Device for TBI

5a. CONTRACT NUMBER

5b. GRANT NUMBER
W81XWH-11-2-0109

5c. PROGRAM ELEMENT NUMBER

6. AUTHOR(S)

Pierre D. Mourad, Ph.D.

E-Mail: pierre@apl.washington.edu

5d. PROJECT NUMBER

5e. TASK NUMBER

5f. WORK UNIT NUMBER

7. PERFORMING ORGANIZATION NAME(S) AND ADDRESS(ES)

University of Washington
Seattle, WA 98107

8. PERFORMING ORGANIZATION REPORT NUMBER

9. SPONSORING / MONITORING AGENCY NAME(S) AND ADDRESS(ES)
U.S. Army Medical Research and Materiel Command
Fort Detrick, Maryland 21702-5012

10. SPONSOR/MONITOR'S ACRONYM(S)

11. SPONSOR/MONITOR'S REPORT NUMBER(S)

12. DISTRIBUTION / AVAILABILITY STATEMENT
Approved for Public Release; Distribution Unlimited

13. SUPPLEMENTARY NOTES

14. ABSTRACT

Improvised explosive devices (IEDs) produce head injuries in nearly a majority of surviving soldiers. Most brain-injured soldiers do not, however, receive the necessary, rapid brain imaging studies as would their civilian counterparts. Instead they are flown to rear-echelon medical service centers such as in Germany for those studies, as well as additional medical care. There exists, therefore, a critical need for robust brain imaging systems at and near the battlefield. This gap in patient care reduces the quality of care and potentially, therefore the quality of life of injured soldiers. This gap also defines a critical need for rugged, field deployable systems capable of imaging injured brain. For a variety of reasons it is reasonable to expect that changes in the stiffness of brain accompany TBI, and that ultrasound-based 'sonoelastic' imaging modalities responsive to some measure of stiffness might offer a useful means for imaging the changes to brain due to TBI. Use of such systems in and near the field should improve clinical outcome for patients suffering from TBI. Our long-term goal is to develop a field deployable brain imaging system, capable of transcranial application, responsive to brain stiffness.

15. SUBJECT TERMS
traumatic brain injury, ultrasound, sonoelasticity, brain imaging

16. SECURITY CLASSIFICATION OF:			17. LIMITATION OF ABSTRACT	18. NUMBER OF PAGES	19a. NAME OF RESPONSIBLE PERSON
a. REPORT	b. ABSTRACT	c. THIS PAGE			USAMRMC
U	U	U	UU	34	19b. TELEPHONE NUMBER *(include area code)*

Table of Contents

INTRODUCTION – subject. Improvised explosive devices (IEDs) produce head injuries in nearly a majority of surviving soldiers. Most brain-injured soldiers do not, however, receive rapid brain imaging studies as would their civilian counterparts. Instead they are flown to rear-echelon medical service centers such as in Germany for those studies, as well as additional medical care. This is because magnetic resonance imaging is unavailable in or near the theatre of war (and a bad idea for many patients because of the presence of metal fragments) and because of the lack reliably operational CT machines at medical centers in Iraq. In the mean time, due to the lack of adequate neuro-imaging, acute neurosurgical care in response to closed TBI often requires a complete hemicraniectomy (removal of one side of the patient's skull) simply to assay the extent and location of injured brain. There exists, therefore, a critical need for robust brain imaging systems at and near the battlefield. Also, more subtle brain injuries are apparent clinically but difficult to definitively diagnose, hence treat. These gaps in patient care reduce the quality of care and potentially, therefore the quality of life of injured soldiers. This gap also defines a critical need for rugged, field deployable systems capable of imaging injured brain.

INTRODUCTION - purpose. For a variety of reasons it is reasonable to expect that changes in the stiffness of brain accompany TBI, and that ultrasound-based 'sonoelastic' imaging modalities responsive to some measure of stiffness might offer a useful means for imaging the gross and subtle changes to brain due to TBI. Use of such systems in and near the field should improve clinical outcome for patients suffering from TBI. Our long-term goal is to develop a field deployable brain imaging system responsive to brain stiffness. Our system would do so through the use of ultrasound applied transcranially.

INTRODUCTION – scope of the research. To met the goal of this proposal we sought to test the following hypothesis: Rodent brain after closed TBI (blast, controlled cortical impact (CCI); ischemic stroke) manifest spatial patterns of endogenous and exogenous tissue displacement, hence patterns of brain-tissue stiffness, sufficient to map and identify the extent of each of hemorrhage, edema, and TAI, as tested via the following iterative aims.

Specific Aim #1: Quantify via histology and MR the spatial position and extent of each of hemorrhage, edema and TAI within each of the blast and CCI models of brain injury.

Specific Aim # 2: Directly measure the intrinsic stiffness of brain tissue of different types: normal gray and white matter; hemorrhagic brain; edematous brain; traumatized axons.

Specific Aim # 3: Use displacement-based ultrasound to image intrinsic brain tissue stiffness of normal versus traumatized rodent brains and their component parts.

KEY RESEARCH ACCOMPLISHMENTS

Specific Aim #1: Quantify via histology and MR the spatial position and extent of each of hemorrhage, edema and diffuse axonal injury (DAI) within each of the blast and CCI models of brain injury, with comparable studies for ischemic stroke.

Task (1): Generate closed TBI (mild and moderate-to- severe) in rats using blast methodology.

Task (2): Generate closed TBI (mild, moderate-to-severe) using CCI methodology in 'mito' mice and in rats and ischemic stroke using an occlusion model in mice.

1,2a) Get approval for the animal models. We here at UW have received UW and ACURO IACUC committee approval as has UVA.

1,2b) Establish the animal models. We here at UW have performed CCI on live mice and rats for purposes of establishing the model. At UW we have also established our ischemic stroke model. UVA has done the same with their CCI animal model.

1,2c) Perform animal-based studies. UW and UVA have performed CCI studies on rats. UW has performed preliminary CCI studies on mito-mice. UW has performed studies on ischemic stroke mice.

Task (3): MR image rodent brains.

3) UVA has performed its first round of MRI studies of CCI rats – Figures 1a,b,c.

Task (4): Immunohistochemical assays.

4) At UW we have performed histological assays of rodent brain after TBI, using Cresyl Violet stains, known to highlight axonal structure. We at UW are waiting for return of the histological samples from NorthWest Zoopath, who is processing the brain tissue (staining and mounting). At UVA they have used their established means of staining damaged brains – Figures 1d,e,f.

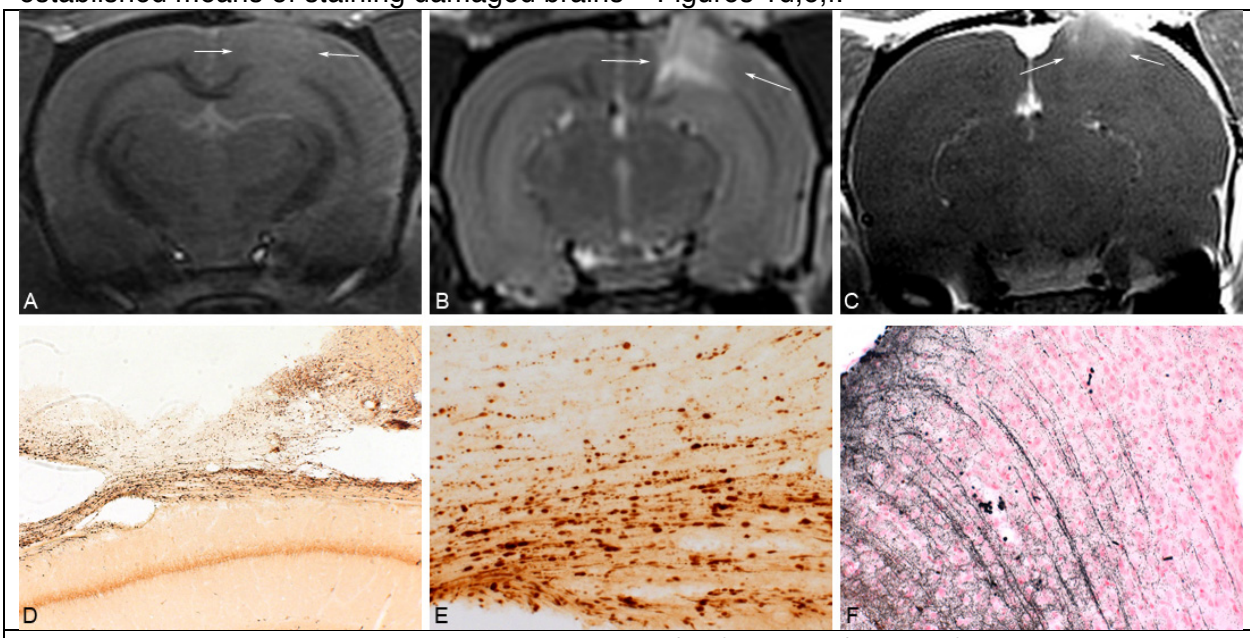

Figure 1. *These MRI and histopathology images (all from UVA) are all from 24 hour post-injury severely injured animals. Below is information on each frame of the plate.* **A:** T1 weighted sequence with arrows demonstrating region of contusion. Notice obliteration of ipsilateral white matter at the site of injury. **B:** T2 weighted sequence demonstrating high signal at site of contusion cavity. Also, notice high signal and loss of ipsilateral white matter. **C:** T2 post-gadolinium contrast demonstrates leaking of contrast into the contusion site, consistent with blood brain barrier disruption. **D:** APP immunohistochemistry at contusion cavity at 50x, demonstrating many traumatically injured axonal profiles. **E:** APP immunohistochemistry at contusion cavity at 200X demonstrating closer view of traumatically injured profiles. **F:** Silver degeneration stain at cortex ipsilateral to contusion demonstrating degenerating dendritic processes.

Specific Aim # 2: Directly measure the intrinsic stiffness of brain tissue of different types: normal gray and white matter; hemorrhagic brain; edematous brain; ischemic brain; traumatized axons.

Task (5): Calibrate indenter system and apply it in vitro as well as to rodent brain tissue samples dominated by one of each of normal gray and white matter; hemorrhagic brain; edematous brain; traumatized axons.

5) UVA has set up indenter system (Figure 2a) and used it on rodent tissue in support of methodology development (Figure 2b). Oscillations in the measurement of rat brain-tissue displacement introduce uncertainty into the brain tissue stiffness measurements we seek from this experiment.

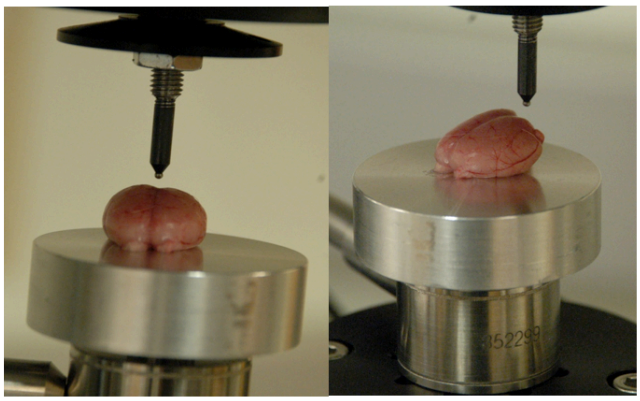

Spherical Indenter centered above superior and inferior Colliculus

A

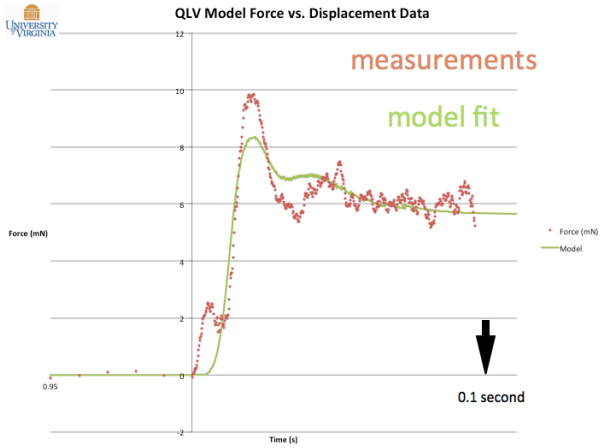

B

Figure 2. Brain-tissue indenting system and first results. (A) This set of photos shows a fresh rat brain on the brain-indentation system. Mild force (milliNewtons) distributed over a square millimeter or two indents the brain. **(B)** The brain rapidly deforms; fitting a mathematical model of that deformation to the measurements, along with assumptions of some brain-tissue properties including calculations of the shape of the deformation will produce estimates of the bulk and shear modulus of the tissue under compression.

After these initial studies UVA has begun to refine their indenter system applied to rodent tissue in support of methodology development exploring in particular the effect of time after euthanasia on inferred brain-tissue stiffness (Figure 3a,b) which they seek to minimize through reducing the time to perform the experiments in part by reducing the number of measurements they seek to get from a given brain. They have also made preliminary measurements with pieces of freshly harvested pig brain (Figure 3c) that yields results (Figure 3d) with likely greater reproducibility whose supporting methodology they can adapt to rat brain.

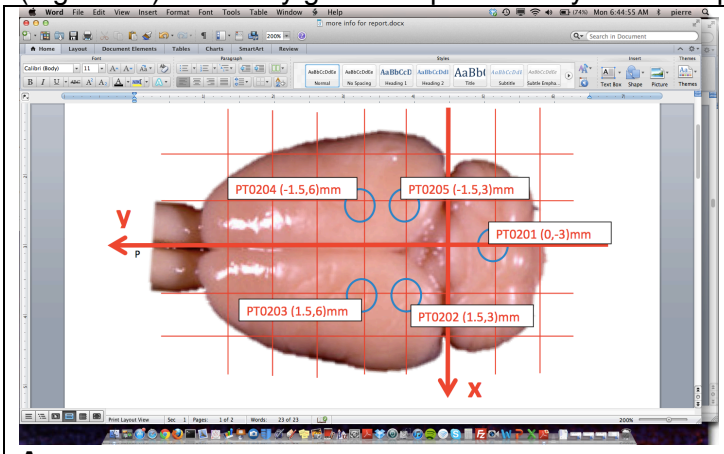

A

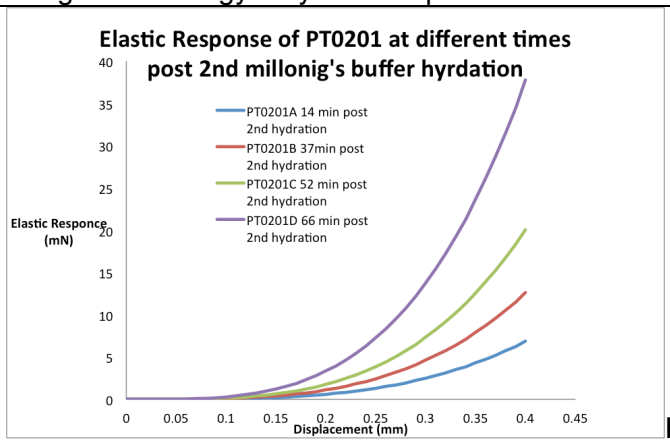

B

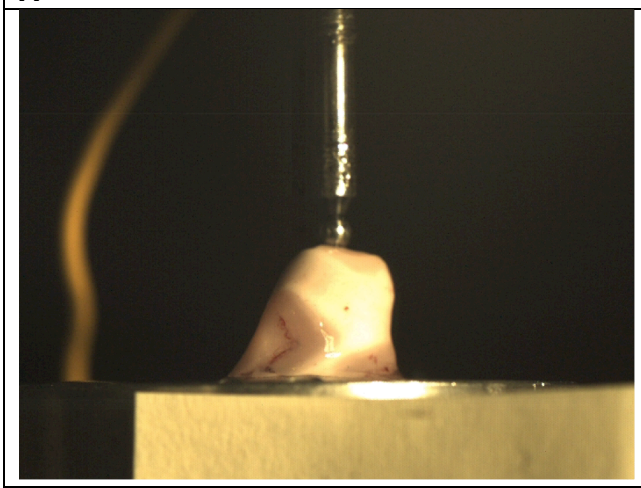

C

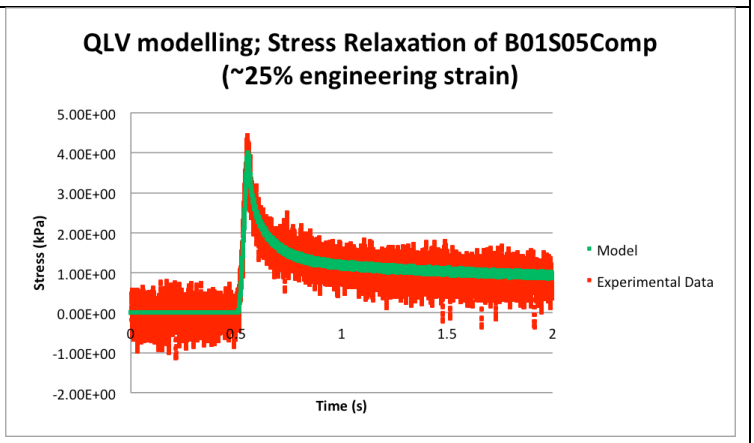

D

Figure 3 shows various indenter results for rat (A, B) and pig (C,D). Figure **(A)** shows a schematic of indenter position measurements while Figure **(B)** shows measurements of rat-brain displacement (horizontal axis) versus measured elastic response in milliNewtons, all as a function of time after euthanasia. For larger displacements (many in a relevant range) there exists a substantial impact of tissue age on the measurements. Figure **(C)** shows a piece of freshly harvest pig brain on our indenter system while Figure **(D)** shows direct measurements of the inferred stress as a function of time after indentation along with the associated model fit used to translate the directly measured elastic response (as in Figure B) to stress. Note the negligible oscillations in these results vs in the comparable rat results (Figure 2 above).

Specific Aim # 3: Use displacement-based ultrasound to image intrinsic brain tissue stiffness of normal versus traumatized rodent brains and their component parts.

Task (6): Optimize commercial ultrasound-imaging device based on measurement of exogenous and endogenous brain palpation.

6) We have established a procedure for optimizing the analysis of images from the commercial ultrasound imaging system, based on exogenous brain palpation by the SSI machine via the acoustic radiation force and subsequent monitoring of the propagation of a shear wave. Figure 4 demonstrates this analysis procedure, along with the accompanying histopathology analysis, for ischemic stroke. Below in Task 8 we show the results of this analysis applied (as here) to ischemic stroke as well as to mild TBI in rats induced by the CCI method.

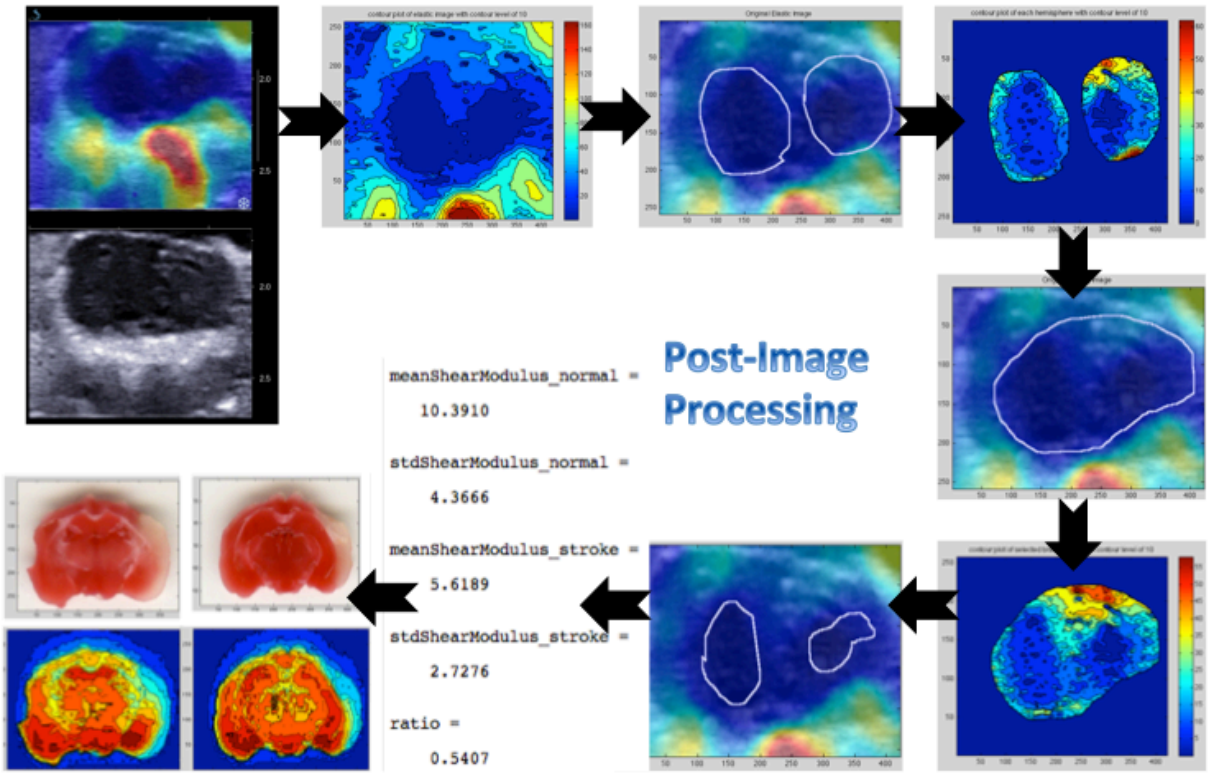

Figure 4. This figure shows examples of raw shear-modulus and B-mode images (upper left-hand corner) and subsequent processing of those images (two different versions here) to define regions of interest that have minimal artifacts in them (bright colors). Analysis of those images produces estimates of the shear modulus in the different hemispheres. The bottom left-hand image shows sample TTC results from the same mouse brain post stroke, where the white portions of brain has suffered ischemic damage to the mitochondria within the brain. Both the shear-modulus imaging and TTC demonstrate changes ipsilateral to middle cerebral artery occlusion (the right-hand side of all images) relative to the contralateral side.

Task (7): Optimize research ultrasound-imaging device based on measurement of exogenous and endogenous brain palpation.

7a) We remain able to generate images of shear-wave propagation using our research ultrasound-imaging device (the VUE system). As noted before, the presence of a discrete lesion significantly complicates the propagation patterns of the diagnostic shear waves (Figure 5, overleaf). We are working through published methods of quantifying the extraction of shear-wave propagation speed from these images, so we can infer local variations in shear modulus.

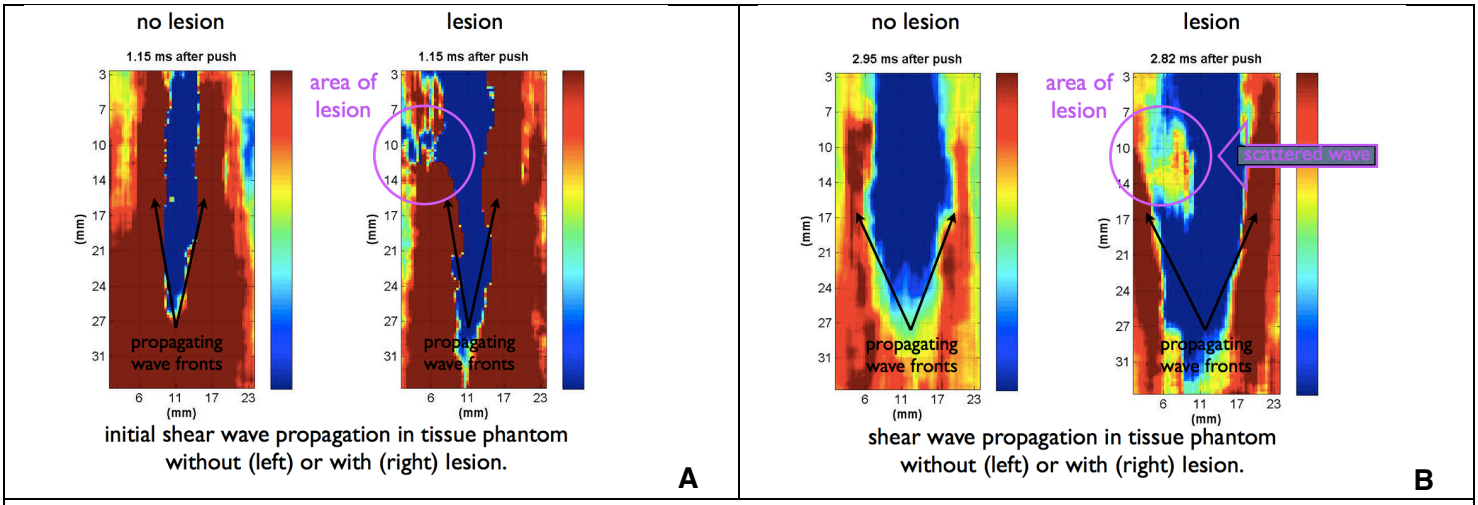

Figure 5. These figures show the propagation of shear wave fronts, in vitro, generated and imaged by our VUE system. The sub-images in each of images A, B on the left come from tissue phantoms without large-scale inhomogeneities. The sub-images on the right in each of images A, B come from a different portion of the otherwise homogeneous tissue phantom that contains a discrete 'lesion' – a volume of tissue phantom with different stiffness than the background. **A.** This figure demonstrates the initial distribution of shear wave fronts 1.15 ms after the initial push generated by the focused diagnostic ultrasound system, which occurs in the center of imaged region. Already apparent is destruction of the portion of the propagating shear wave at the location of the inhomogeneity. **B.** This figure demonstrates the subsequent evolution of the propagating shear wave fronts after an additional 1.8 ms. While complex, here we focus here on the effect of the lesion on the propagating shear-wave: the destruction of the initially propagating shear wave front as well as the backscatter of an additional shear-wave front from the lesion. Such spatial variations in shear-wave propagation can translate into errors in inferred tissue stiffness, errors we seek to eliminate through our analysis.

7b) We have tested on control rats an exogenous brain palpation system based on vibrating brain with focused ultrasound, whose methodology we review in Figure 6.

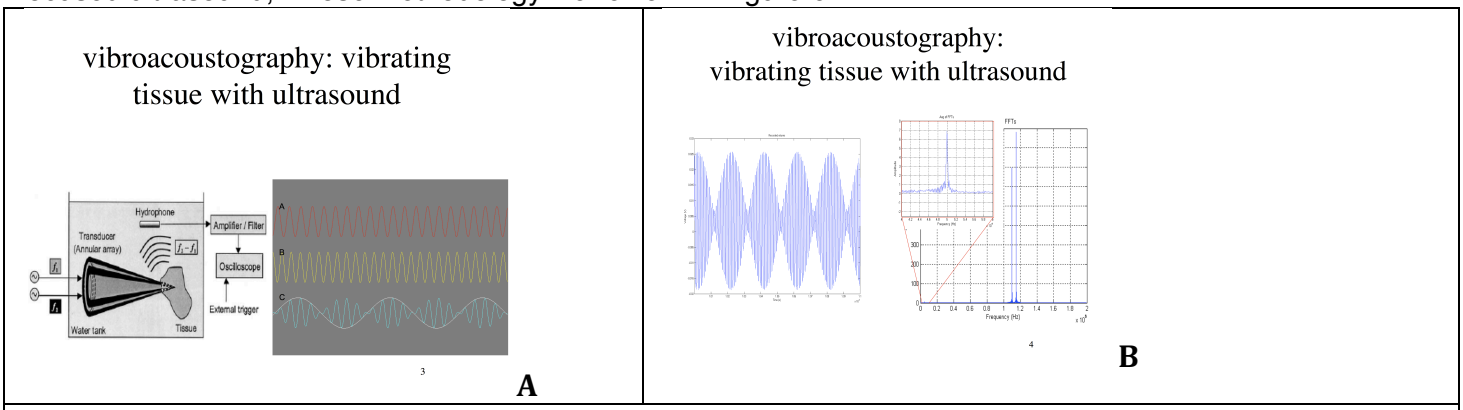

Figure 6. A. In vibroacoustography, a dual-transducer device ('transducer (annular array)') emits two, separate pulses of ultrasound at two different, but close frequencies – pulse train 'A' and 'B'. The ultrasound sources have been designed so that their foci overlap within the material of interest (tissue phantom or brain, here) through use of this intense focused ultrasound (iFU). At the focus, high frequency oscillations move the tissue slightly; their beat frequency generates a low-frequency emission, itself sampled from a separate hydrophone placed either in the water tank or within the iFU source itself for *in vivo* applications. **B.** This figure shows real data rather than the conceptualization of Figure 1A. Specifically, the left-hand figure of B shows a measured waveform demonstrating the net signal generated by the overlapping separate, high frequency iFU signals, whose two, dominating spectral peaks appear in the right-hand figure of B. The low-frequency waveform overlying on the high-frequency signals in the left-hand figure of B matches the observed beat frequency shown in the spectrum (inset of figure of B). We anticipate that the amplitude of these low-frequency emissions vary with the presence versus absence of traumatized brain, either averaged over a hemisphere of a rodent brain, or, in a point-wise fashion for the brain's of larger animals and of humans. Vibroacoustography may therefore offer a new means of creating *images* of TBI in humans.

We show results from one of our first few untreated rats (Figure 7a) as well as averages of the 'diagonal' values of the acoustic emissions for these same rats (Figure 7b). These results are not yet robustly reproducible, however, likely because of the sensitivity of this method to the anatomical placement of the focus of ultrasound that creates the vibroacoustography effect. This same sensitivity should be a bonus when we try this out on rats with TBI.

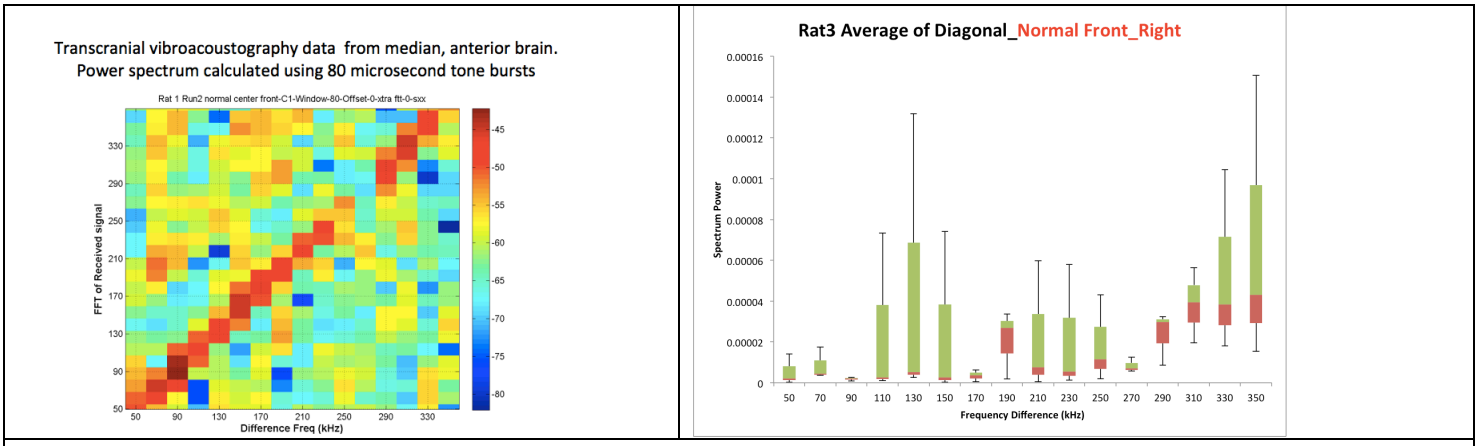

Figure 7. Power spectrum of acoustic emissions due to vibroacoustography applied transcranially to untreated rats: (A) shows an example of the entire spectrum while (B) shows the average of the diagonal across all five untreated rats within different frequency bins. The horizontal axis marks the choice of difference frequency generated at the focus of the vibroacoustography source. The vertical axis marks the sampling frequency of the acoustic emissions. Most applications of vibroacoustography produce dominant acoustic emissions at the same frequency as the difference frequency of the incident ultrasound such as here. We don't yet always achieve results with a strong diagonal response, the subject of on-going work.

7c) We have started to collect endogenous and exogenous brain-tissue imaging results from mito-mice subjected to TBI via CCI. These mice have the unique property that the mitochondria within the neurons in their brain fluoresce when healthy (Figure 8). Using them we will be able to assay for subtle white-matter damage that standard histopathological techniques can miss.

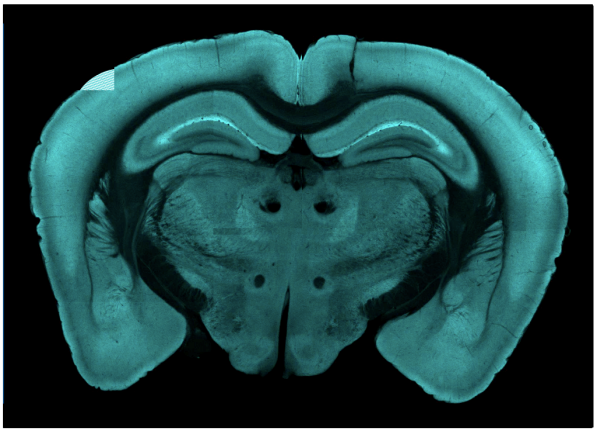

A

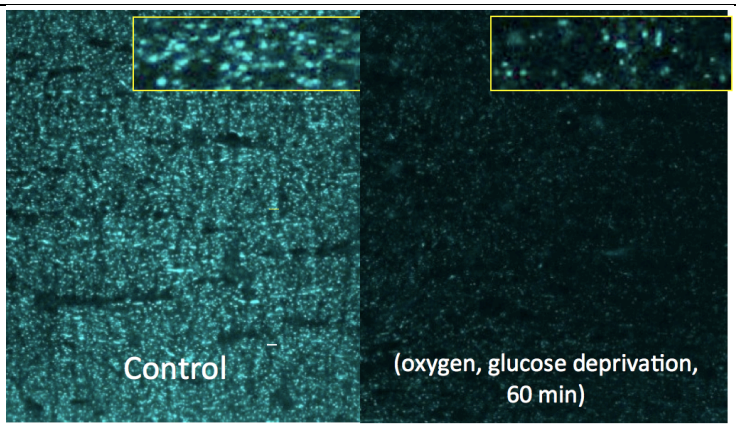

B

Figure 8. (A) This figure shows a coronal slice of a brain of a 'mitomouse' - a mouse whose neuronal mitochondria fluoresce when healthy and reduce or loose their fluorescence when damaged or dead, respectively. **(B)** This figure shows slices of the optic nerves of two mitomice, in work published by our UW colleagues (Morison and Murphy). Each subimage shows both low-power and high-power microscopy views of this tissue. The control tissue has been processed normally while the other tissue has been subjected to deprivation of both oxygen and glucose for 60 minutes. Relative to the control, the damaged tissue has suffered loss of mitochrondrial function. For the present proposal we intend to assay for standard histological damage as well as damage to the white matter (using fluorescence microscopy), a common problem in TBI, which we will assay for the first time using mitomice.

To optimally process our endogenous ultrasound imaging results results as well as demonstrate the potential utility of this means of imaging brain in humans, we have turned to an existing data set derived from a human TBI case. This human data consists of B-mode ultrasound image (Figure 9a) from which we have derived tissue-pulsatility images (Figure 9b,c) to compare against a corresponding CT image (Figure 9d,e). These preliminary comparisons support the hypothesis that pulsatility images may offer an ultrasound-based means of imaging TBI in humans. Since the skull should not pulsate more than a micron, but appear to pulsate on scales of tens of microns, we infer that movement of the transducer causes this effect. We will mitigate this effect by developing pulsatility images of human brain (and rodent brain in separate studies) *relative to the artifactual motion of skull.* We will also use micropositioners to hold our ultrasound scan heads for our mouse studies.

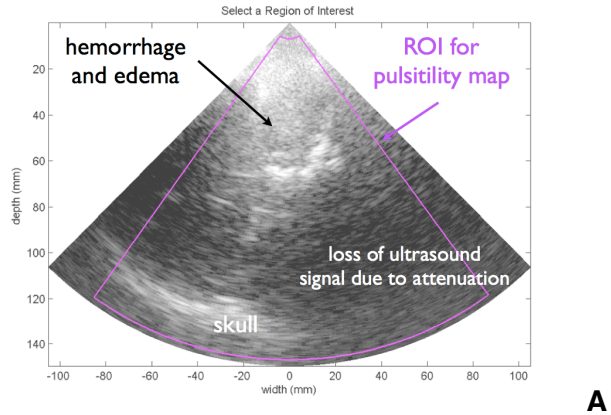

A

Figure 9. (A) We have transformed transcranially derived B-mode ultrasound images within a Region of Interest (ROI) into **(B)** unannotated and **(C)** annotated images of the pulsatility [e.g., local instantaneous displacement] of brain tissue (in units of microns for the color bar) caused by pulsatile flow of blood into the brain. We compare these images with axial CT images of the same brain here shown both unannotated **(D)** and annotated **(E),** with interpretation by UW neuroradiologist (Norm Beauchamp), who identified focal hemorrhage surrounded by a rim of edema. Hemorrhagic tissue appears to maximally pulsate while edematous brain appears to minimally pulsate in patterns consistent with CT.

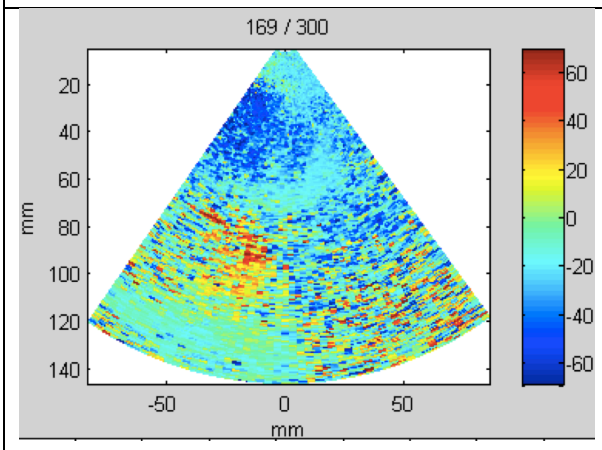

B

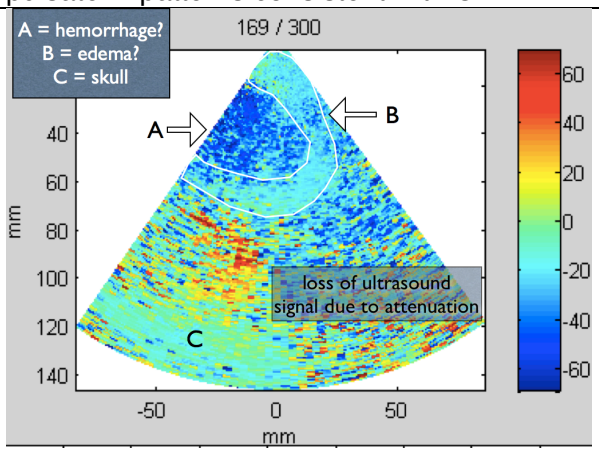

E

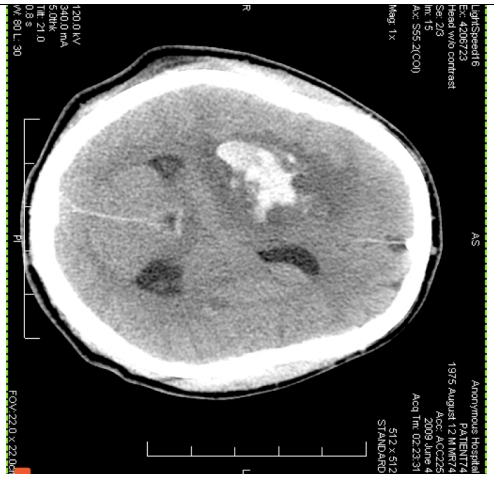

F

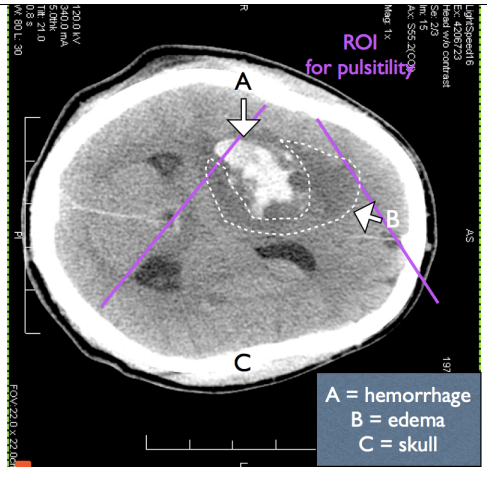

G

Task (8): Image normal versus damaged rodent brains with commercial and research ultrasound devices.

(8a) We have finished use of the commercial SSI system *without any modification* on ischemic stroke mice. While we could not image brain damage with that commercial system, we could detect it (Figure 10a,b,c). We have written that work up in a paper (sent in separately with this report). It is now under review at *Journal of Ultrasound in Medicine*.

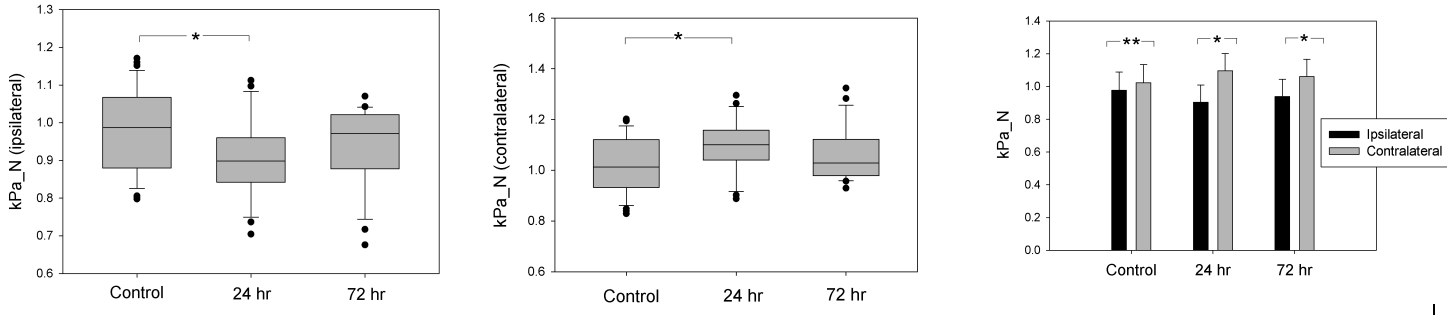

Figure 10 demonstrates our ability to detect changes in intra-hemispheric brain stiffness despite imaging artifacts at different levels of statistical significance [* = p<0.01; ** = p<0.05] (left) This figure shows how the normalized ipsilateral shear modulus [larger values, stiffer tissue] varies between control mice, mice 24 hours or 72 hours after occlusion of their middle cerebral artery [hence MCAO mice] in the ipsilateral hemisphere. Interhemispheric brain-tissue stiffness after MCAO decreases then normalizes, likely due to initial reduction in blood flow that overwhelms initial edema formation followed by increased contribution of edema to hemisphere-integrated stiffness. **(center)** Contralateral to MCAO, the normalized contralateral hemisphere stiffens 24 hours after stroke, then normalizes, likely due to initial decrease in contralateral blood flow followed by 'diaschesis' – contralateral development of edema. **(right)** Interhemispheric differences in normalized tissue stiffness for each of control as well as 24 and 72 hours after MCAO. There exist minor differences between intra-hemispheric values of brain-tissue stiffness for the control mice, while there exist substantial differences between hemispheres at 24 and 72 hours post stroke, with reductions in brain-tissue stiffness within the hemisphere of brain directly subjected to ischemia and subsequent edema.

(8b) In the meantime we have performed 'image' analysis on our mild CCI rats comparable to what we performed on our stroke mice – Figure 11. These results demonstrate changes in hemispherically averaged shear modulus for each of the hemispheres. We see an ipsilateral decrease in shear modulus relative to control by 24 hours after CCI injury. This is consistent with edema formation after CCI, a well-established phenomenon in this animal model for TBI. Unexpectedly, we also see a contralateral increase in shear modulus relative to control by 24 hours after CCI injury, consistent with the possible reduction of blood flow contralateral to injury that is sometimes observed in stroke patients and consistent with what we observed for our stroke animals, and also consistent with observations of TBI patients, but has not been reported for this animal model. Our UVA colleagues will measure ipsilateral and contralateral perfusion in their CCI rats to test this hypothesis.

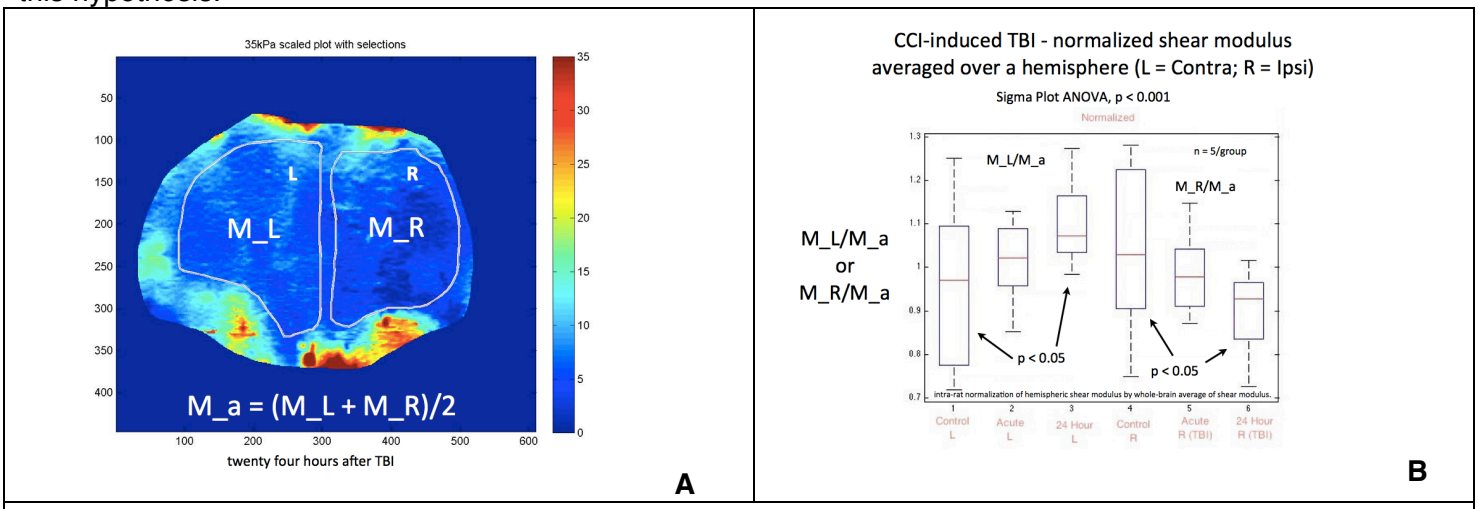

Figure 11. Coronal slice of 'image' of brain-tissue stiffness of rat brain 24 hours after mild TBI induced via the CCI method and associated statistics. We collected shear-modulus images from rats after mild TBI induced by CCI (0.5mm indentation) into the right hemisphere of their brains through a small cranial window. Imaging artifacts continue to manifest in these images, here as hot colors around the periphery of the image. Nonetheless, in this example, the right hemisphere has a lower mean shear modulus (M_R) than the left hemisphere (M_L). We calculated the average shear modulus M_a then used it to normalize the shear moduli for each hemisphere of the control, acute (within one hour) and 'chronic' – 24 hours after CCI.

Task (9): Compare images of strain, and of bulk and shear modulus of brain with histological and MR-based images of hemorrhage, edema, ischemia and TAI.

9) NA

Task (10): Compare images of strain, and of bulk and shear modulus of brain tissue with images of bulk and shear modulus derived by assigning directly measured values of bulk and shear modulus to portions of histological images.

10) NA

Task (11): Generate first-order specifications for a device capable of imaging TBI in humans.

11) NA

REPORTABLE OUTCOMES

(1) We have observed changes in hemispherially-averaged brain-tissue stiffness in ischemic brain tissue within mice consistent with physiological changes in brain observed in rodent models of ischemic stroke as well as in patients with ischemic stroke. These observations include ipsilateral edema formation and short-term contralateral reduction in blood flow and longer-term contralateral edema formation.

(2) We have developed a plausible new means of detecting TBI based on generation and detection of focal, low-frequency vibration within brain via a process known as vibroacoustography.

(3) We have preliminary data from humans consistent with the hypothesis that endogenous brain-tissue palpation created by the pulsatile blood flow within brain can highlight edema and hemorrhage within aTBI patient

(4) We have observed changes in hemispherially-averaged brain-tissue stiffness in mild to moderate TBI generated by the controlled cortical impact (CCI) method with rats consistent with physiological changes in brain observed in rodent models of TBI as well as in patients with TBI. These observations include ipsilateral edema and hemorrhage formation (observed in rodents and in patients) and short-term contralateral reduction in blood flow (observed in patients but not in rodents).

(5) We have made progress on the image-analysis methods necessary to resolve intra-hemispheric changes in brain due to TBI.

(6) We have made progress on our direct means of measuring brain-tissue stiffness, data that will give us ground-truth measurements of that stiffness for comparison with our ultrasound-based means of imaging brain-tissue stiffness variations in the context of TBI.

CONCLUSIONS

We have generated evidence supportive of the hypothesis that ultrasound-derived brain-tissue stiffness imaging using exogeneous 'palpation' of brain with diagnostic ultrasound can successfully detect changes in rat brain caused by both ischemic stroke and in TBI. We have also generated evidence supportive of the hypothesis that endogeneous palpation of brain by cerebral blood flow can highlight hemorrhage and edema found within the brain of a TBI patient. We have also made substantial progress towards achieving the capability of making direct measurements of brain-tissue stiffness in rats *ex vivo.* Taken together, these results among the others reported here demonstrate that we are making appropriate progress, relative to our milestones, towards creation and demonstration of the ability of ultrasound to image TBI with a field-deployable device.

REFERENCES

Xu JS, Chu S, Lee RJ, Paun M, Yao A, Murphy S, Mourad PD. Evidence of diaschisis after ischemic stroke through ultrasound-based elastography. Submitted to *J. Ultrasound in Medicine.* [see the appendix for a copy of this paper]

APPENDIX

The following pages contain the text, figures, etc associated with a paper we have submitted recently to the Journal of Ultrasound in Medicine, cited above.

Evidence of diaschisis after ischemic stroke from ultrasound-based elastography

Zinnia S. Xu[1]; Rona J. Lee[2], B.S.; Stephanie S. Chu[1]; Anning Yao[1]; Marla K. Paun[3], B.S.; Sean P. Murphy[2], Ph.D.; Pierre D. Mourad[1,2,3], Ph.D.

[1]Department of Bioengineering, Univ. of WA; [2]Department of Neurological Surgery, Univ. of WA; [3]Applied Physics Laboratory, Univ. of WA

Corresponding Author:
Pierre D. Mourad
Department of Neurological Surgery
University of Washington
Box 356470
Seattle WA 98195-6470

(main) 206-543-3570
(fax) 206-543-6785
(office & voicemail) 206-543-9125
(email) pierre@apl.washington.edu

Running Title: Observing diaschisis with sonoelastography

ABSTRACT

Objectives: Diaschisis, defined as transhemispheric ischemia, edema development, and reduced blood flow, can occur as a result of stroke, complementing comparable changes in the ipsilateral hemisphere. Here ultrasound elastography, an imaging process sensitive to fluid content in tissue, was used to study changes in individual hemispheres after transient ischemic injury.

Methods: Ultrasound elastographic images of mouse brain were collected 24 hours and 72 hours after middle cerebral artery occlusion. The shear modulus of both ipsilateral and contralateral brain hemispheres for these mice were measured and compared to corresponding values of control animals.

Results: At 24 hours (but not 72 hours) after induction of ischemic stroke, there was a significant decrease in shear modulus in the ipsilateral hemisphere($P < 0.01$) and a significant increase in shear modulus in the contralateral hemisphere compared to that of control animals($P < 0.01$). Significant differences were also evident between ipsilateral and contralateral shear modulus values at 24 and 72 hours after infarction ($P < 0.01$; $P < 0.01$, respectively).

Conclusion: The differences between shear moduli of animals with stroke for 24 and 72 hours likely reflect the initial development of edema and reduction of cerebral blood flow known to develop ipsilateral to ischemic infarction, as well as the known initial reduction of blood flow and subsequent development of edema in the contralateral hemisphere (diaschisis). Thus, elastography offers a possible method to detect subtle changes in brain after ischemic stroke.

KEYWORDS

Cerebral Stroke; Ultrasound; Diaschisis; Elastography; Middle Cerebral Artery Occlusion

INTRODUCTION

Reduction of cerebral blood flow after stroke produces changes in the ipsilateral hemisphere and induces subtle effects in the contralateral hemisphere or "diaschisis" (1). Physiological phenomena associated with diaschisis include a "significant decrease in regional cerebral blood flow of the contralateral hemisphere" after MCAo (middle cerebral artery occlusion), as shown in cats (2). Further, in addition to characterization of the progression of edema on the ipsilateral hemisphere, (3) others have observed changes in fluid content in the contralateral hemisphere after ischemic injury through MR images as early as nine hours after occlusion (4).

Elastography has been used for many years to detect tissue stiffness and is growing in importance for breast cancer diagnoses (5). Here we have used a particular version of ultrasound elastography that is sensitive to the average fluid content in tissue, in order to investigate ipsilateral and contralateral changes in brain after ischemic injury in mice (6).

MATERIALS AND METHODS

Middle Cerebral Artery occlusion

Male C57BL/6 mice (25-30g) were used for the 45-minute middle cerebral artery occlusion (MCAo). Anesthesia was induced by inhalation of 3% isoflurane and maintained using 1.5-2% isoflurane. Body temperature was monitored throughout the surgery using a rectal probe and maintained at 36-38°C using a heating blanket. A midline incision was made on the ventral surface of the neck. The right common carotid artery was isolated and ligated; after which a 12mm long, 6-0 nylon filament was introduced and advanced up through the internal carotid artery and into the middle cerebral artery. Mice were kept under anesthesia for the entire duration of the 45-minute occlusion. After the occlusion, the filament was pulled back and removed from the artery to allow for reperfusion. Cerebral blood flow in the area was monitored during the occlusion and reperfusion using a Laser Doppler (MoorLab – Laser Doppler Perfusion Monitor). Mice were sacrificed either 24-hours or 72-hours later by cervical dislocation.

Control animals did not undergo surgical preparation. Pilot studies by us performed over the years have shown no difference in brain structure as shown by MRI and histopathology between control animals that received the sham surgery and control animals that received no surgical procedure. We therefore chose to use controls without surgery for this imaging study. There were a total of thirteen control mice and sixteen mice that underwent the MCAo procedure: eight sacrificed after 24 hours and eight sacrificed after 72 hours. All procedures were approved under University of Washington Institutional Animal Care and Use Committee (UW IACUC).

Ultrasound Image Acquisition

Anesthesia was induced in the animals by inhalation of 3% isoflurane and maintained during data acquisition at 1-2% isoflurane. Hair was removed from the head to decrease attenuation of ultrasound caused by air trapped within the hair. The skull and skin were left intact. A custom made polyvinyl alcohol (PVA) standoff **(7)** was used to maintain an optimal distance of ~30mm between the transducer and the bottom of the mouse brain. The standoff was placed between the mouse and the transducer to maintain optimal distance between the transducer and the mouse brain. Polysonic (Cone Instruments, Solon, OH) multi-purpose ultrasound gel was used between the mouse and the standoff and between the standoff and the transducer for better conduction of the ultrasound waves. The transducer was moved along the anteroposterior axis of the brain. Multiple coronal images were taken from the front, middle, and back sections of the brain. Image artifacts associated with the skull were avoided as much as possible when selecting images from SWE mode. Approximately 3 - 6 images were taken from each section of the brain.

An Aixplorer Multiwave Ultrasound System (SuperSonic Imagine, Aix-en-Provence, France) with its linear SL 15-4 MHz transducer was used to measure the shear modulus of brain tissue in our animals. The transducer's imaging frequency ranged between 4.0-15.0 MHz, with a standard center frequency of 8.5 MHz. Two types of image were collected, ShearWave Elastography (SWE) and B-mode.

B-mode assessed the two-dimensional anatomy of the brain region from the echoes returning from tissue of different density (8). SWE mode shows absolute tissue elasticity displayed per pixel. In SWE mode, the penetration depth was ~30mm (6). Imaging was performed within a range of 0-180 kPa in an unblinded fashion to minimize gross imaging artifacts associated with the surrounding tissue and skull (figure 1), since typical brain values of shear modulus lie between 2.7 – 13.6 kPa. This method therefore blinded the user to the imaging of the brain itself (9,10).

2,3,5-Triphenyltetrazolium chloride (TTC) staining

Mouse brains were removed after cervical dislocation and cut into eight 1mm coronal sections. Slices were stained with 0.1% 2,3,5-Triphenyltetrazolium chloride (Sigma) in PBS for 40 minutes to one hour, at room temperature, in the dark (figure 2). They were then fixed in 4% formalin and stored at 4°C. Mice that showed no infarct through TTC stain were excluded from the study.

Ultrasound Image Analysis

Ultrasound images were chosen for analysis from the same section of brain (front, middle, back) that showed infarct after TTC staining. We chose one out of the approximately five ultrasound images per mouse that had minimal imaging artifact as defined above (figure 3A).

All post-processing of the images was done using MATLAB. In post-processing, the entire brain region was manually selected using free-form selection from the SWE-mode image obtained from the Aixplorer (figure 3B). Because the SWE-mode image shows the elastographic image on top of the B-mode image, the operator can select the portion of brain within the cranium based on the structure of the skull seen in B-mode. After the selection, the elastographic image of the selected brain region was compressed to an elasticity range of 0-35 kPa (from 0-180kPa) for increased visualization and contrast within the brain, which tends to have a lower shear modulus than the skull (see figure 3C). The ipsilateral and contralateral hemispheres of the brain were

then manually selected directly from the elastographic image of the brain (Figure 3D). These regions were selected with care to avoid skull and artifacts from the skull, distinguished by areas of high shear modulus that extend from outside the brain into the brain region (Figure 3D). The shear moduli of the two hemispheric selections were averaged to obtain a mean shear modulus for each hemisphere.

This feature extraction analysis was performed three times for each image in a blinded fashion to ensure that there was no operator bias. The images were coded so that the operator did not know whether the image was from a control, 24-hour or 72-hour stroke mouse.

TTC Image Analysis

The TTC-stained brain slices were scanned. The operator who performed the TTC image analysis was blinded to whether the mouse had a stroke for 24 or 72 hours. Using free-form selection in MATLAB, we first selected the entire portion of the image that contained brain. We then selected the region of brain containing an infarct. The number of pixels in the infarct was divided by the number of pixels within the entire brain. With this information the percentage of brain that contained an infarct was calculated. The selection of the infarct area was done three times for every image and the percentage of brain with infarct was averaged over the three images.

Data Analysis

Mean shear modulus values were normalized for each individual mouse. The mean shear modulus (G) of each hemisphere was divided by the average of the two hemispheres for each mouse:

$$G_{N_{ipsi}} = \frac{G_{ipsi}}{\frac{G_{ipsi}+G_{contra}}{2}}$$

$$G_{N_{contra}} = \frac{G_{contra}}{\frac{G_{ipsi}+G_{contra}}{2}}$$

The normalized shear modulus (G_N) reports the value of the shear modulus of each hemisphere for each given mouse relative to the average value across the entire brain. Note that a normalized value of one means that contralateral and ipsilateral hemispheres have the same average shear modulus.

Student's t-test was used to compare the average shear modulus for each hemisphere (ipsilateral and contralateral) for three populations: control, 24-hour, and 72-hour mice. The t-tests were calculated between respective hemispheres (contralateral or ipsilateral) among the three populations to see if the mean shear modulus differed significantly between populations. Student's t-tests were also performed on the data for ipsilateral and contralateral hemispheres for each population to identify interhemispheric differences.

Boxplots showing the spread of normalized mean shear modulus values from control, 24-hour and 72-hour mice were prepared for each hemisphere in Sigmaplot.

RESULTS

Percentage of stroke-damaged tissue

The area of infarct for 72-hour animals (mean=15.2%) did not vary in a statistically significant fashion from the area of infarct for the 24-hour animals (mean=10.9%; P=0.20).

Normalized shear modulus of hemispheres

Figure 4A and Table 1 shows that 24-hour animals had significantly decreased ipsilateral shear modulus compared to control animals ($P<0.01$). There was no difference between ipsilateral 72-hour stroke and control animal shear-modulus values (P=0.09). Also, there was no difference between ipsilateral 72-hour and 24-hour stroke animal shear modulus values (P=0.13).

The contralateral hemisphere of 24-hour stroke animals showed a significant increase in elasticity when compared to the control population ($P<0.01$) (Figure 4B). At 72 hours, the stroke and control populations exhibited no difference ($P=0.09$); nor was there a difference between contralateral hemisphere elasticity values at 24 versus 72 hours after stroke ($P=0.13$).

Figure 5 shows that there exists a difference between ipsilateral and contralateral shear modulus at 24 and 72 hours post-stroke with $P<0.01$. There was also a weak difference in the interhemispheric shear modulus for the control animals ($P=0.04$).

DISCUSSION

Our observations include a weak but statistically significant difference ($P = 0.04$) between the stiffness measures of the two hemispheres of control brain. This observed difference is more significant for the interhemispheric stiffness of brains for mice 24 and 72 hours after stroke, where $P < 0.01$. We have therefore chosen to make our assertions of statistical significance at the more stringent p-value of 0.01. This relatively weak difference for control animals could have arisen due to asymmetries in delivery of the focused ultrasound pulse generated by our system and/or could reflect a real, but weak inter hemispheric difference in blood content between each hemisphere, due to the asymmetric input of blood from the heart into the brain.

Comparison to other measures of brain-tissue stiffness

Previous work describing magnetic resonance elastography (MRE) has shown similar estimates of shear modulus (9,10). Kruse et al. has reported the stiffness of white matter as 13.6 kPa and grey matter as 5.22 kPa in a study of 25 healthy people (9), while Green et al reported findings that white matter measured 3.1 kPa and grey matter measured 2.7 kPa in a study of five healthy males (10). Moreover, recent work by Mace et al. using a research version of the clinical ultrasound imaging machine we have reported average values of shear modulus from rat brain ranging between 2-25 kPa, with an average of 12 kPa (11).

While our studies did not distinguish between white and grey matter of the brain, our ultrasound elastographic measurements of tissue stiffness (4.32 kPa, control ipsilateral and 4.49 kPa, control contralateral) are within the values noted for MRE and research sonoelastic machines.

Changes in the ipsilateral hemisphere

In animals 24 hours after stroke, shear moduli of the ipsilateral hemispheres were significantly less than those of control animals. This is likely due to ischemia caused directly by the occlusion as well as the rapid development of edema (4). According to Gotoh and Asano, edema in the ipsilateral hemisphere can start developing a few hours after MCAo, increasing until it reaches a maximum at around 2-3 days (3). Edema slows the propagation of shear waves, thereby directly affecting the shear modulus of the tissue (6). Ischemic brain edema results initially from cell swelling (cytotoxic edema) caused by depleted energy substrates in brain cells by ischemia. Eventually vasogenic edema also develops, caused by increased blood vessel permeability (12). The decrease in ipsilateral elasticity reported here is also consistent with the work of Rousseaux and Steinling, who found mean cerebral blood flow (CBF) values in stroke subjects to be generally lower than those of control subjects in the ipsilateral hemisphere (13).

In animals 72 hours after stroke, the mean ipsilateral shear moduli were not significantly different from that of control animals. One possible explanation is that brain edema ipsilateral to stroke reaches a maximum at 2-3 days after ischemic injury and then begins to decrease (3). Therefore, the average stiffness of ipsilateral brain at 72 hours may have decreased back to baseline because of a combination of reduced edema relative to at 24 hours plus continued ischemia.

Changes in the contralateral hemisphere

We hypothesize that the observed increase in contralateral hemispheric tissue elasticity for the 24-hour animals arose due to a reduction in contralateral cerebral blood flow (1,13). At 72 hours, the values of elasticity of the brains of stroke animals, of contralateral hemisphere, are no different than that of control animals. Observations by Gotoh et al. show that edema develops in

the contralateral hemisphere following infarction and reaches a peak within 2-3 days of infarction (3). We hypothesize that development of edema decreases the overall tissue elasticity, likely accounting for the difference seen between contralateral tissue stiffness 24-hour and 72-hour animals.

Future work

Changes in the distribution of fluids within brain (blood; edema) have been observed after stroke, based on MRI and PET as well as direct analysis of tissue, in both ipsilateral and contralateral hemispheres (1,3,4,12,13). Using ultrasound-based elastography that is sensitive to the average fluid content of tissue (6) we have observed changes in brain stiffness. These changes are consistent with the hypothesis that ultrasound-based elastography is sensitive to diaschisis. Successful testing of these hypotheses will motivate future imaging work in humans after stroke. Moreover, recent work with a research version of the clinical ultrasound system (11) showed the ability of shear wave imaging to resolve intracranial brain structure, further increasing its potential utility. For example, the portable and economical aspect of the technology may prove to have an impact on the management and detection of stroke in areas where CAT scans and magnetic resonance imaging are not readily available or appropriate.

ACKNOWLEDGEMENTS

We received funding from the Congressionally Directed Medical Research Program (CDMRP)

REFERENCES

1. Andrews RJ. Transhemispheric diaschisis. A review and comment. *Stroke*. 1991;22:943-949

2. Han DH, Jung HW, Lee SH, Kim HJ, Choi KS, Sim BS. Acute cerebral infarction and changes of regional cerebral blood flow (rcbf) following experimental middle cerebral artery (mca) occlusion. *Neurol Res*. 1988;10:203-212

3. Gotoh O, Asano T, Koide T, Takakura K. Ischemic brain edema following occlusion of the middle cerebral artery in the rat. I: The time courses of the brain water, sodium and potassium contents and blood-brain barrier permeability to 125i-albumin. *Stroke*. 1985;16:101-109

4. Izumi Y, Haida M, Hata T, Isozumi K, Kurita D, Shinohara Y. Distribution of brain oedema in the contralateral hemisphere after cerebral infarction: Repeated mri measurement in the rat. *J Clin Neurosci*. 2002;9:289-293

5. Garra BS. Elastography: Current status, future prospects, and making it work for you. *Ultrasound Q*. 2011;27:177-186

6. Tanter M, Bercoff J, Athanasiou A, Deffieux T, Gennisson JL, Montaldo G, Muller M, Tardivon A, Fink M. Quantitative assessment of breast lesion viscoelasticity: Initial clinical results using supersonic shear imaging. *Ultrasound Med Biol*. 2008;34:1373-1386

7. Fromageau J, Brusseau E, Vray D, Gimenez G, Delachartre P. Characterization of pva cryogel for intravascular ultrasound elasticity imaging. *IEEE Trans Ultrason Ferroelectr Freq Control*. 2003;50:1318-1324

8. Mourad PD. Biological effects of ultrasound. *Encyclopedia of Electronics and Electrical Engineering*. 1999;2:368-386

9. Kruse SA, Rose GH, Glaser KJ, Manduca A, Felmlee JP, Jack CR, Jr., Ehman RL. Magnetic resonance elastography of the brain. *Neuroimage*. 2008;39:231-237

10. Green MA, Bilston LE, Sinkus R. In vivo brain viscoelastic properties measured by magnetic resonance elastography. *NMR Biomed*. 2008;21:755-764

11. Mace E, Cohen I, Montaldo G, Miles R, Fink M, Tanter M. In vivo mapping of brain elasticity in small animals using shear wave imaging. *IEEE Trans Med Imaging*. 2011;30:550-558

12. Rosenberg GA. Ischemic brain edema. *Prog Cardiovasc Dis*. 1999;42:209-216

13. Rousseaux M, Steinling M. Crossed hemispheric diaschisis in unilateral cerebellar lesions. *Stroke*. 1992;23:511-514

TABLE AND FIGURE LEGENDS

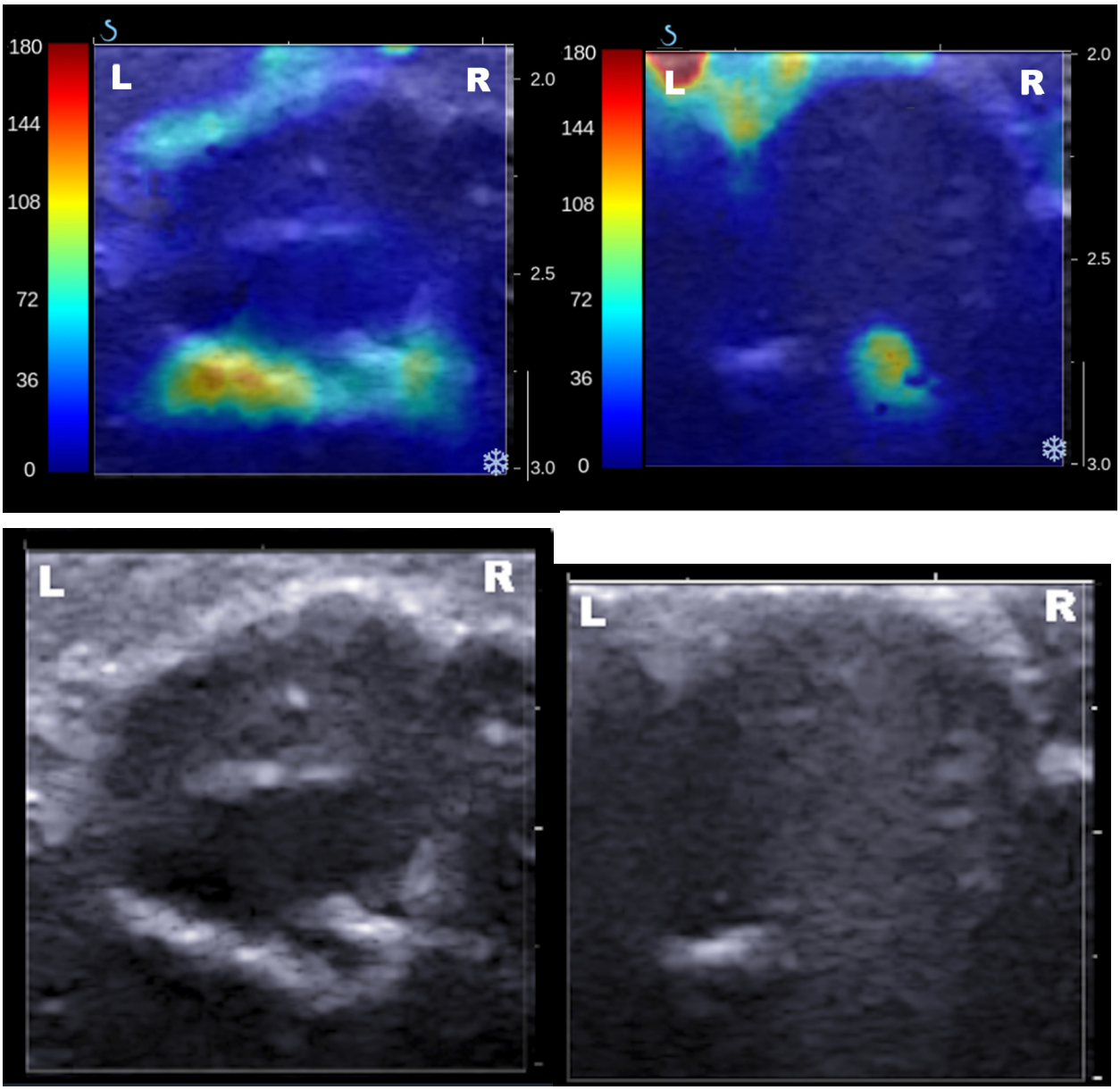

Figure 1. These images show significant imaging artifact (hot colors) diffusing intracranially, where the white line shows the position of the skull, as shown on B-mode images.

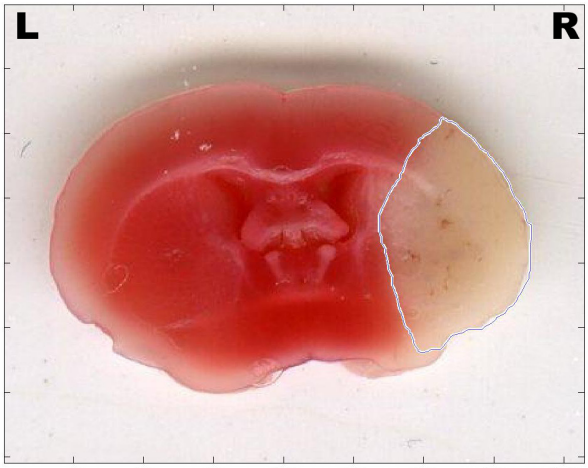

Figure 2. Representative TTC image with stroke region highlighted in white. This image shows a TTC image of a stroke taken after 72 hours.

3A

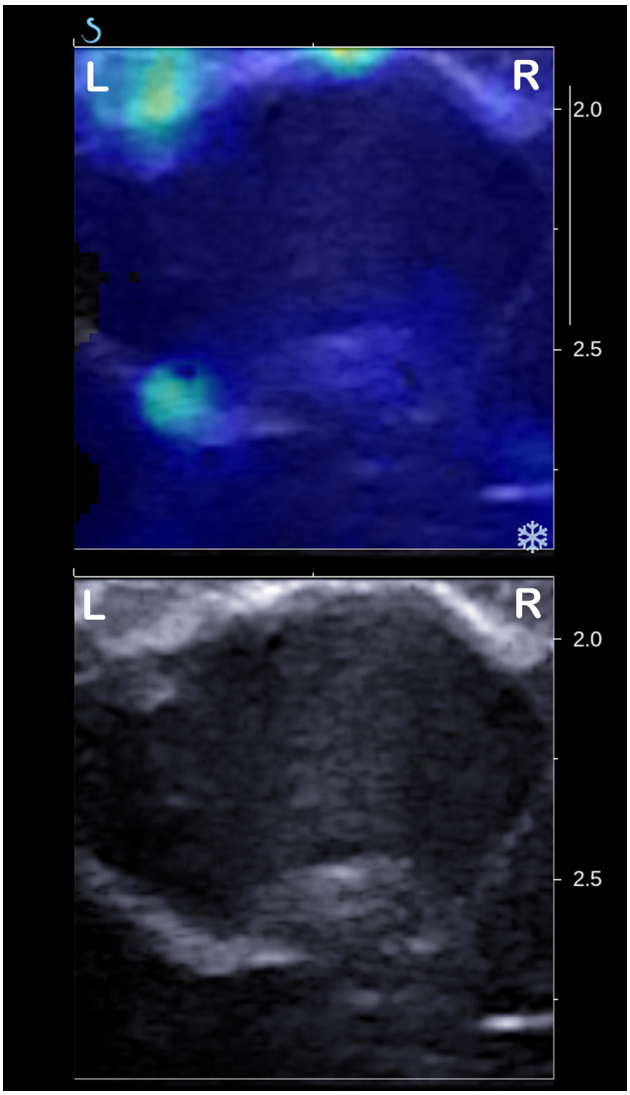
L
R
2.0
2.5
L
R
2.0
2.5

B

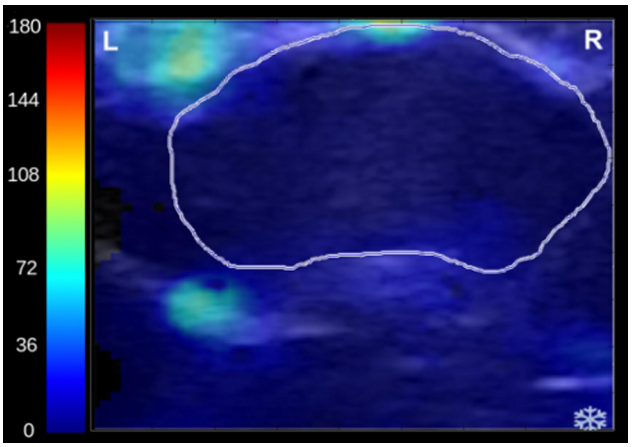
180
144
108
72
36
0
L
R

C

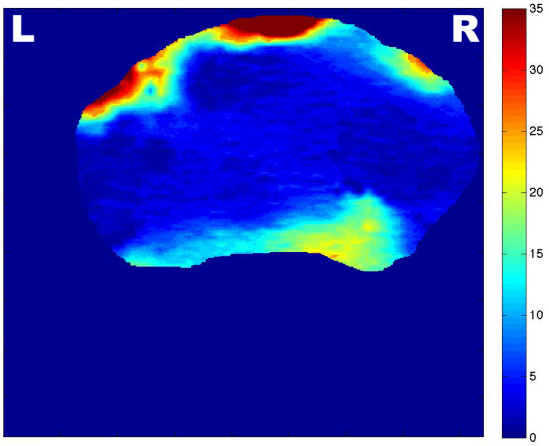
L
R
35
30
25
20
15
10
5
0

D

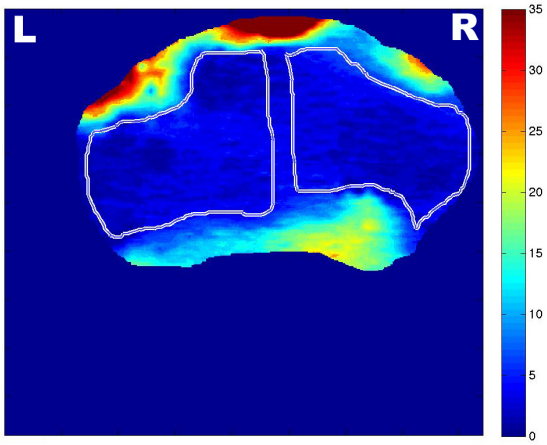
L
R
35
30
25
20
15
10
5
0

Figure 3. Stroke Image Processing (A) Aixplorer images in SWE mode (top) and B-mode (bottom). (B) The brain was selected from the elastographic image displayed on top of the corresponding B-mode image. (C) The elastography image of the entire brain was scaled to 35 kPa to enhance the contrast. Regions of high stiffness are indicative of image artifacts. (D) The hemispheric regions to be analyzed were selected manually by the operator in order to avoid skull and artifacts (hot color regions associated with large values of shear modulus).

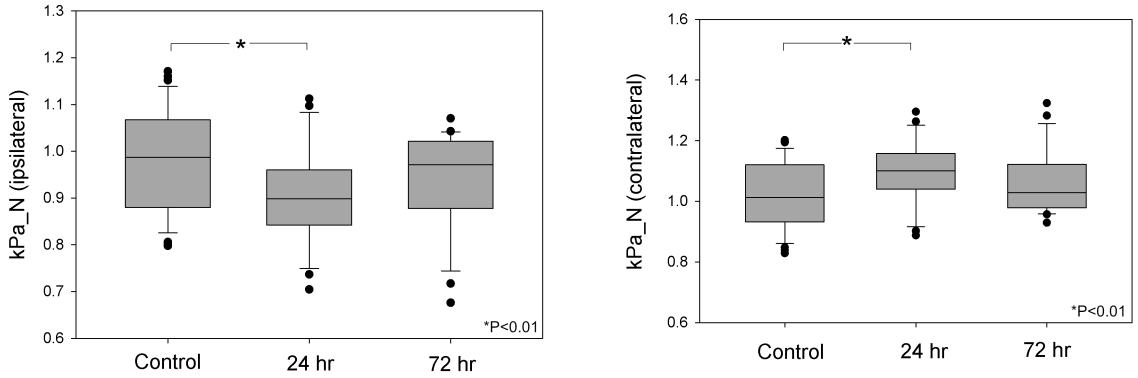

Figure 4. (A) Normalized Ipsilateral Shear Modulus for control, 24-hour and 72-hour mice. (B) Normalized Contralateral Shear Modulus for control, 24-hour and 72-hour mice. *P<0.01.

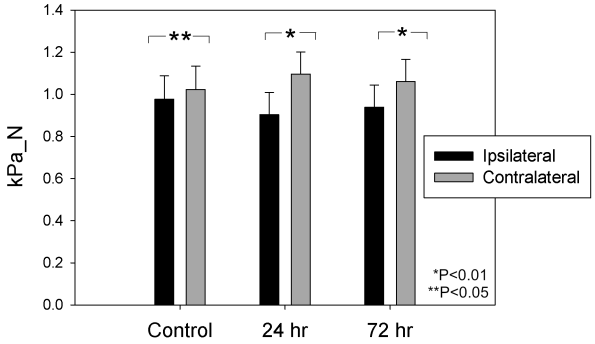

Figure 5. Comparison of normalized mean shear modulus of ipsilateral and contralateral hemisphere for all three populations: Control, 24-hour and 72-hour mice. *P<0.01 **P=0.04.

	Control	24 hours	72 hours
Ipsilateral (Non-normalized; kPa)	4.32 + 1.44	3.85 + 0.96	3.66 + 1.02
Contralateral (Non-normalized; kPa)	4.49 + 1.32	4.86 + 1.79	4.23 + 1.49
Ipsilateral (Normalized)	0.98 ± 0.11	0.90 ± 0.10	0.94 ± 0.10
Contralateral (Normalized)	1.02 ± 0.11	1.10 ± 0.10	1.06 ± 0.10

Table 1. Non-normalized (kPa) and normalized mean and standard deviation for mean shear modulus values of three populations: control, 24-hour and 72-hour.